SU(N) fractional Instantons

Jorge Luis Dasilva Golán[ab,*] **and Margarita García Pérez**[a]

[a]*Instituto de Física Teórica UAM-CSIC, Nicolás Cabrera 13-15, Campus de Cantoblanco.*
E-28049, Madrid, Spain

[b]*Departamento de Física Teórica, módulo 15, Universidad Autónoma de Madrid, Cantoblanco.*
E-28049, Madrid, Spain

E-mail: jorge.dasilva@uam.es, margarita.garcia@csic.es

We present our study of a set of solutions to the $SU(N)$ Yang-Mills equations of motion with fractional topological charge. The configurations are obtained numerically by minimizing the action with gradient flow techniques on a torus of size $l^2 \times (Nl)^2$ with twisted boundary conditions. We pay special attention to the large N limit, which is taken along a very peculiar sequence, with the number of colors N and the magnetic flux m selected respectively as the n-th and $n - 2$ terms of the Fibonacci sequence. We discuss the large N scaling of the solutions and analyze several gauge invariant quantities as the Polyakov loops. We also discuss the so-called Hamiltonian limit, with one of the large directions sent to infinity, where these instantons represent tunneling events between inequivalent pure gauge configurations.

---

*Speaker

1. Introduction

The search for solutions to the Yang-Mills (YM) equations of motion on the hypertorus has had a long history starting with the seminal works of 't Hooft in the early 80's [1]. The freedom to select boundary conditions, corresponding to gauge potentials periodic up to gauge transformations, leads to the appearance of new topological classes, implying, in particular, the possibility of having fractional topological charge. In this paper, we will consider so-called twisted boundary conditions (TBC) whereby, under the shift by a torus period, the gauge potential transforms as:

$$A_\mu(x + l_\nu \hat{e}_\nu) = \Omega_\nu(x) A_\mu(x) \Omega_\nu^\dagger(x) + i\, \Omega_\nu(x) \partial_\mu \Omega_\nu^\dagger(x), \tag{1}$$

with $\Omega_\nu(x)$ taken as $SU(N)$ matrices constrained by the consistency relation:

$$\Omega_\nu(x + l_\mu \hat{e}_\mu)\, \Omega_\mu(x) = \exp\{i 2\pi n_{\nu\mu}/N\}\, \Omega_\mu(x + l_\nu \hat{e}_\nu)\, \Omega_\mu(x), \tag{2}$$

and $n_{\mu\nu}$ a non-trivial antisymmetric tensor of integers defined modulo N, known as twist tensor.

One interesting property that TBC introduces is that the topological charge Q is no longer bounded to be an integer, but it is quantized in terms of the twist tensor as [2, 3]:

$$Q = \frac{1}{16\pi^2} \int d^4x \mathrm{Tr}\left(F_{\mu\nu}(x)\widetilde{F}_{\mu\nu}(x)\right) = \nu - \frac{\vec{k} \cdot \vec{m}}{N}, \tag{3}$$

where $m_i = \epsilon_{ijk} n_{jk}/2$ is the spatial part of the twist, the so-called magnetic flux, while $k_i = n_{0i}$ is dual to the electric flux characterizing the Hilbert space in a Hamiltonian set-up.

Following these considerations, we summarize in this work our search for $SU(N)$ instanton solutions with fractional topological charge $Q = 1/N$ [4]. We are particularly interested in those corresponding to a Hamiltonian set up: $\mathbf{R} \times \mathbf{T}^3$, with $\mathbf{T}^3$ a 3-dimensional torus endowed with TBC. In this limit, the fractional instantons we will present have a well defined interpretation as tunneling events interpolating between two different pure gauge configurations at $x_0 \rightarrow \pm\infty$. Fractional charge solutions of this type were first obtained numerically for $SU(2)$ [5, 6] and later generalized to $SU(N)$ [6, 7] for various choices of the twist tensor (vortex-like solutions have also been obtained [8, 9]). In this proceedings, we focus on new $SU(N)$ solutions that have been obtained on asymmetrical tori with sizes $l_1 = l_2 = l/N$, $l_3 = l$, and $l_0 = sl$, with s a free parameter that is taken to infinity in the Hamiltonian limit. The number of colors is taken along the Fibonacci sequence as $N = F_n$, and the electric and magnetic fluxes are given respectively by: $\vec{k} = (0, 0, -\bar{m})$, and $\vec{m} = (0, 0, m)$, with $m = F_{n-2}$ and $\bar{m} = (-1)^n F_{n-2}$; it is easy to check, using eq. (3), that this choice leads to topological charge $Q = 1/N$, for $\nu = (-1)^{n+1} F_{n-4}$.

Let us explain the reasons behind these very particular choices. The logic behind our geometry follows the idea of volume independence under TBC, see i.e. [10–12] and references therein. With our choice of twist, the color and spatial degrees of freedom get entangled, and the torus periods in the twisted directions become effectively enlarged by a factor of N. Hence, the effective dynamics of our spatially asymmetric torus corresponds, in the large N limit, to a symmetric one with period l in all three spatial directions. On the other hand, our selection of twist aims to avoid the appearance of tachyonic instabilities and center symmetry breaking in the large N limit [13–17]. It has been conjectured that in order to avoid these problems the flux m should be scaled with N [18] and this is
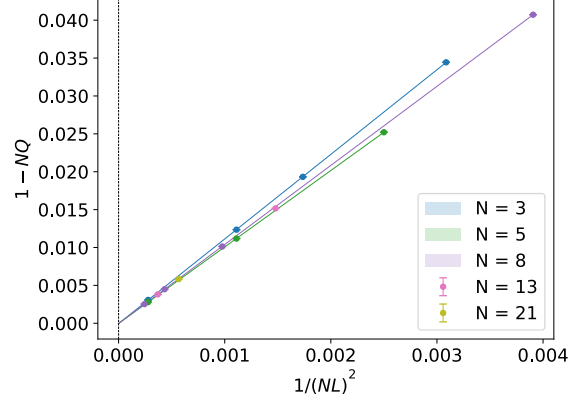
Figure 1: Continuum extrapolation of $1 - NQ$ with $a^2 = 1/(NL)^2$ corrections.

optimally achieved by taking m and the number of colors as the $n-2$ and n-th terms of the Fibonacci sequence [19, 20].

We have analyzed several gauge groups: $N = 3, 5, 8, 13, 21$. Using gradient flow minimization, numerical solutions are obtained on lattices of size: $sNL \times L^2 \times NL$. Fixing the lattice spacing through: $a = l/NL$, our discretization corresponds to a continuum torus with periods $sl \times (l/N)^2 \times l$ with TBC implemented in the usual way.

For each value of N (and for different lattice spacings) we have computed the total action, the electric and magnetic parts of the action (computed to test self-duality), and the topological charge. Selecting different values of the lattice spacing, we were able to extrapolate these quantities to the continuum. As an illustration, figure 1 shows the extrapolation of $1 - NQ$ that agrees with the continuum result up to one part in 10^4.

In what follows, section 2 discusses the action density of the solutions, comparing them with the constant curvature fractional instantons that are know to exist for certain values of the torus aspect ratios [2, 21]; section 3 analyzes Polyakov loops and we conclude with a brief summary of results.

2. Action density

We have determined the density profiles (in units of $8\pi^2$) obtained by integrating the 4-dimensional action density along two or three spatial directions:

$$s_{\mu\nu}(x_\mu, x_\nu) \equiv \left(\prod_{\rho \neq \mu, \nu} \int_0^{l_\rho} dx_\rho \right) s(x), \tag{4}$$

$$s_\mu(x_\mu) \equiv \left(\prod_{\rho \neq \mu} \int_0^{l_\rho} dx_\rho \right) s(x). \tag{5}$$

In the analysis of the large N scaling of these profiles, an inspiring guide has been the case of constant curvature fractional charge solutions that are known to exist for certain values of the torus periods. Following the general construction presented in ref. [21], it is easy to obtain solutions of this type with gauge group and twist parameters taken in the Fibonacci sequence – a complete
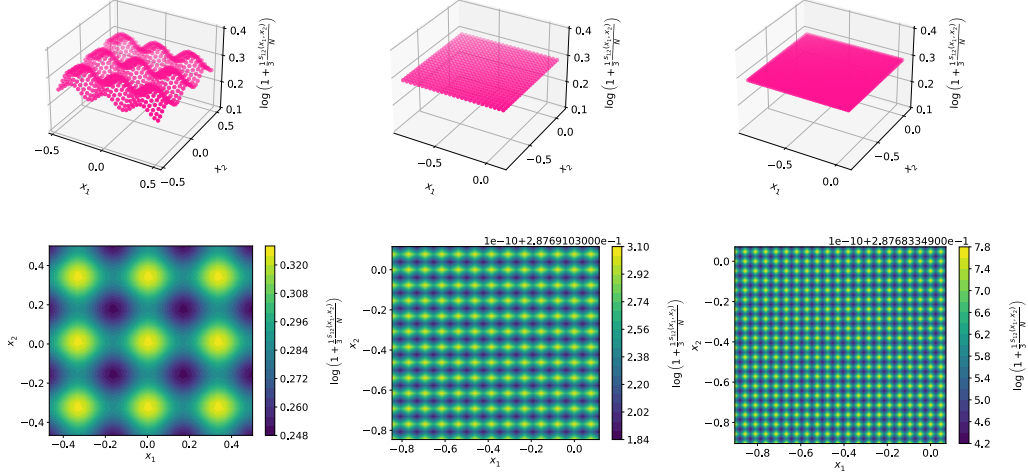
Figure 2: Profile $l^2 s_{12}(x_1, x_2)/N$ as a function of x_1/l and x_2/l. In order to make the structure more visible, the quantity displayed is $\log(1 + l^2 s_{12}(x_1, x_2)/(3N))$. Gauge groups are, from left to right: $SU(3)$, $SU(13)$, and $SU(21)$.

deduction can be found in ref. [4]. The important result is that taking $m = F_{n-2}$ and $N = F_n$, solutions to the Yang-Mills self-duality equations exist for any value of l_0 satisfying:

$$l_0/l = \frac{F_{n-m+1} F_{n-m}}{F_n^2 F_m F_{m-1}} \tag{6}$$

where we have scaled $l_1 = l_2 = l/F_n$, and set $l_3 = l$. For these solutions the profiles are flat and satisfy: $l^2 s_{12}(x_1, x_2)/N = 1$; $l^2 N s_{03}(x_0, x_3) = l/l_0$; and $lN s_0(x_0) = l/l_0$. In the limit $n \to \infty$, the maximal value of the time extent is attained for $l_0/l = \varphi^{-3} \sim 0.236$, with φ the Golden Ratio. We will see below how our solutions compare with these estimates.

Let us start with the analysis of 2-dimensional profiles. Fig. 2 shows $l^2 s_{12}(x_1, x_2)/N$ as a function of the coordinates in the twisted plane for several values of N; each configuration has been replicated N times in each direction for the display. Profiles are practically flat in this plane, with the level of flatness increased as the value of N grows, becoming almost independent of the two short directions. In addition, the hight of the profiles matches very well the one expected for the constant curvature solution which for the quantity displayed in the plot is $\log(1 + 1/3) = 0.287682$.

Figure 3 shows the profiles of $N l^2 s_{03}(x_0, x_3)$, for $l_0 = l_3 = l$ ($s = 1$). In this case, the solutions are localized, developing a maximum and decaying fast far away from the center. Notice that the hight of the peak is not far from the value expected for the constant curvature solution with maximal value of l_0/l, i.e. $l/l_0 \sim 4.427$; we will come back to this point later on.

We can obtain a more quantitative comparison if we look at the 1-dimensional energy profiles, obtained by integrating over the 3 spatial coordinates. Figs. 4a and 4b show the value of $N l s_0(x_0)$ as a function of x_0/l for various values of N and $s = 1$ and $s = 2$ respectively. It is clear that, once the overall factor N is set, the remaining N dependence is rather small, and all curves tend to
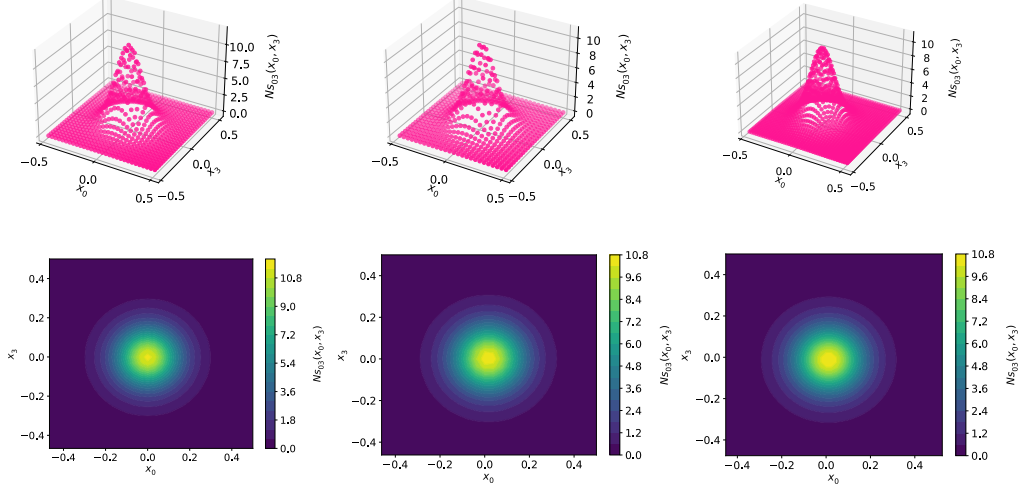
Figure 3: Profile $Nl^2 s_{03}(x_0, x_3)$ as a function of x_0/l and x_3/l. Gauge groups are, from left to right: $SU(3)$, $SU(13)$, and $SU(21)$. We have taken $l = 1$ to set the scale.
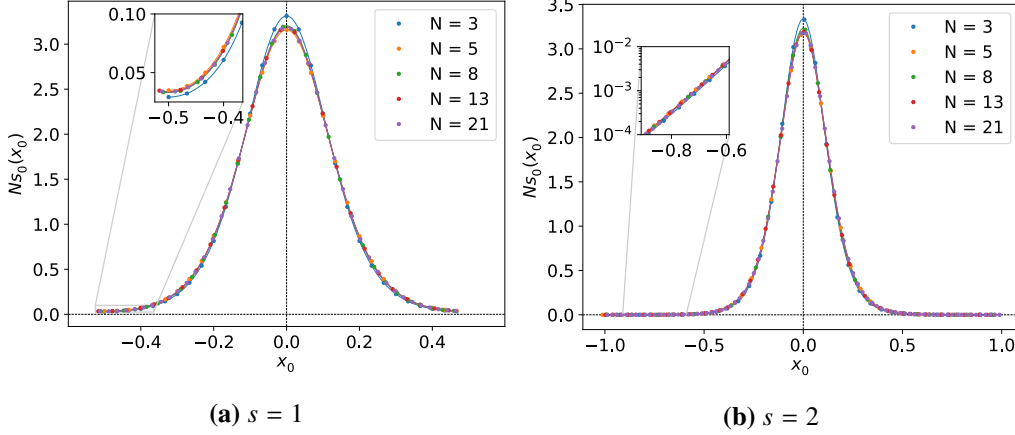

(a) $s = 1$ **(b)** $s = 2$

Figure 4: Time dependence of the energy density profile for various gauge groups N and time extents $l_0 = sl$, with $s = 1$ and 2. The inset in the right plot is in logarithmic ($y-$) scale to show that the decay in the tails is exponential in time.

a universal behavior. Moreover, enlarging the time direction with a factor $s = 2$ does not change drastically the shape of the profile, except at the tails where it decays exponentially.

To compare our solution with the constant curvature one, we have generated several minimum-action configurations starting at $l_0 = 0.25l$ (close to the Fibonacci case), and growing up to $l_0 = l$. The resulting energy density profiles are shown in figure 5. The solutions change rapidly at the beginning, but beyond $l_0 \sim 0.5l$ they remain unchanged except at the tails where, in the large l_0/l limit, they decay exponentially. We believe this exercise is very clarifying, going in the line of interpreting these solutions as deformations of the constant curvature ones [21, 22].

One final test that can be done concerns self-duality. To test this, we have computed the energy
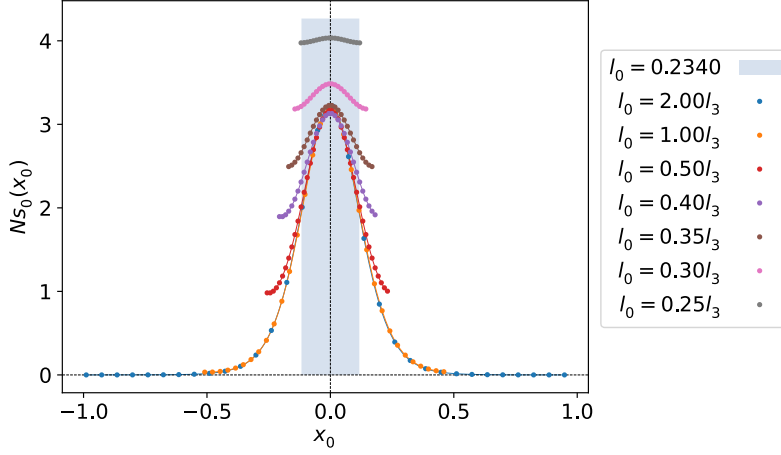
Figure 5: Several solutions for different values of time extent l_0 compared to the constant curvature one with $l_0/l = \varphi^{-3} = 0.236$.

profiles in one direction, but separating the computation of the electric and magnetic contributions as $\mathrm{Tr}(F^2_{\mu\nu})$, with μ and ν fixed. The result for several values of N and various lattice spacings is shown in fig. 6. The degree of self-duality is very high in all configurations and tends to increase as the continuum limit $a = l/(LN) \rightarrow 0$ is approached.

3. Polyakov loops

In this section we will analyze the Polyakov loops, and, based on the Hamiltonian limit discussed in the introduction, we will check the interpretation of the fractional instantons as tunneling events interpolating between two pure gauge configurations.

Let us start the discussion by defining $P_\mu(x)$ as ($1/N$ times) the trace of the Polyakov loop winding the torus once in direction μ:

$$P_\mu(x) = \frac{1}{N}\mathrm{Tr}\left(\mathrm{P}\exp\left\{-\,\mathrm{i}\int_0^{l_\mu}\mathrm{dx}_\mu\mathrm{A}_\mu(x)\right\}\Omega_\mu(x)\right) \equiv |\mathrm{P}_\mu(x)|\,\mathrm{e}^{\mathrm{i}\phi_\mu(x)}. \tag{7}$$

Notice that this definition is slightly different from the case with periodic boundary conditions, needing the insertion of a $\Omega_\mu(x)$ matrix to preserve gauge invariance. The periodicity properties of the loop derived from this definition amount to:

$$P_\mu(x + l_\nu\hat{e}_\nu) = e^{i\frac{2\pi n_{\mu\nu}}{N}}P_\mu(x). \tag{8}$$

Once the twist is fixed, we can use gauge invariance to bring the three spatial $\Omega_i(x)$ matrices to a constant form, the so-called twist eaters, that satisfy the consistency relation:

$$\Gamma_1\Gamma_2 = e^{i\frac{2\pi m}{N}}\Gamma_2\Gamma_1, \tag{9}$$

$$\Gamma_3\Gamma_i = \Gamma_i\Gamma_3, \text{ for } i = 1, 2. \tag{10}$$

It is trivial to check that $A_i = 0$ is consistent with these boundary conditions and leads to Polyakov loops given by:

$$P(\gamma, w_1, w_2, w_3) = \frac{1}{N}\mathrm{Tr}\left(\Gamma_1^{w_1(\gamma)}\Gamma_2^{w_2(\gamma)}\Gamma_3^{w_3(\gamma)}\right), \tag{11}$$
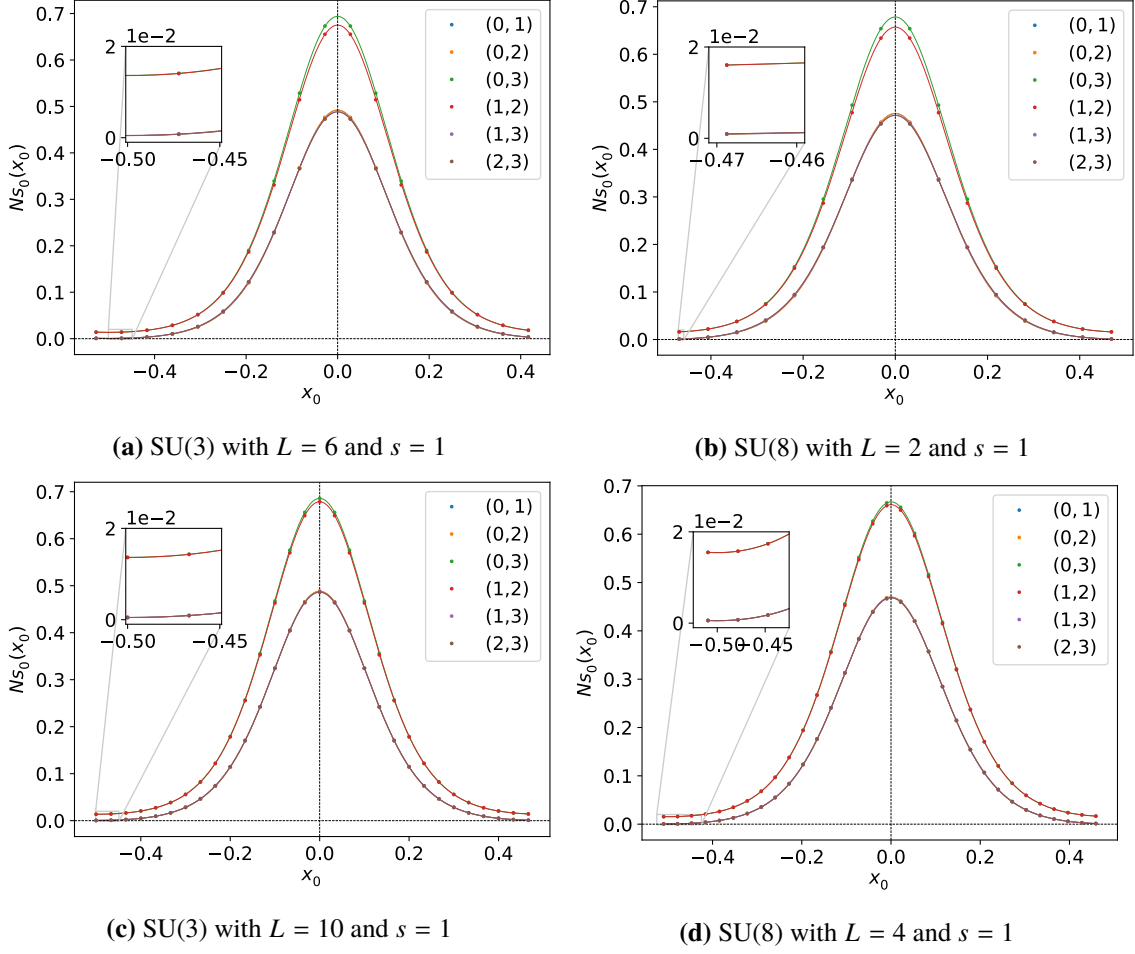
Figure 6: Electric and magnetic components of the energy density as a function of x_0, obtained by integrating $\mathrm{Tr}(F_{\mu\nu}^2)$ for different values of N and lattice spacings.

where γ is a closed curve and $w_i(\gamma)$ is the winding in the ith direction, defined modulo N. In our particular case, this implies $P(\gamma, 0, 0, 1) = z_3$ and $P(\gamma, w_1, w_2, 0) = 0$, unless w_1 and w_2 are both equal to zero (mod N), meaning that flat connections can be characterized with the value of the non-trivial Polyakov loop in the third direction.

Starting from a pure gauge configuration at $x_0 = -\infty$, our choice of space-time twist combined with the periodicity condition of the Polyakov loop, leads to another pure gauge configuration at $x_0 = +\infty$ that differs from the former in the value of the holonomy in the x_3 direction by a a factor $\exp\{2\pi i n_{30}/N\}$. In what follows we will compare these expectations to our numerical results.

The two holonomies in the short torus directions remain all the time very small and tend to zero as we go in the time direction far from the instanton center (details are given in ref. [4]). At all values of t, the modulus of the two loops tends to decrease as the value of N grows.

On the other hand, fig. 7 displays from top to bottom: the change of phase in P_3 (multiplied by N/n_{30}) and the modulus $|P_3|$, all of them for tori with $l_0 = 2l_3$. The results converge to universal curves for all values of N that match well the expectations. First, far from the instanton center, P_3 approaches an element of the center group, with modulus 1 and phase equal to $2\pi/N$ times an
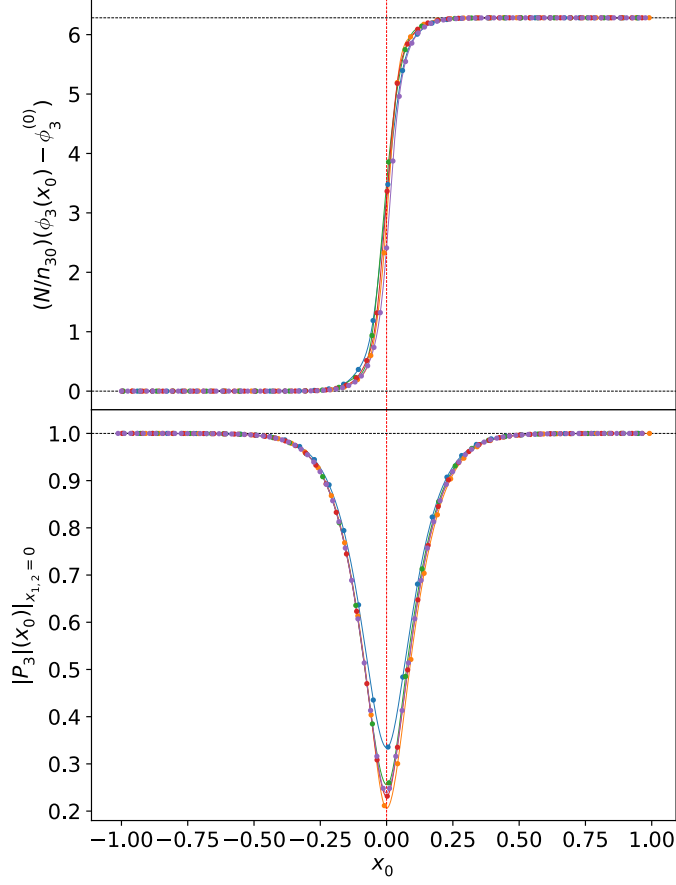
Figure 7: We display as a function of time, for $l_0 = 2l_3 = 2l$, and from top to bottom: the change of phase of P_3 multiplied by N/n_{30} and its modulus, both evaluated at $x_1 = x_2 = 0$.

integer. Moreover, the jump from $x_0 = -\infty$ to $x_0 = +\infty$ is as expected for our choice of space-time twist, with phases at both ends differing by a factor $2\pi n_{30}/N$.

4. Summary

In this work, we have obtained a new type of $SU(N)$ instanton configuration on the hypertorus with the special property of having fractional topological charge $Q = 1/N$, which is a direct consequence of the choice of twisted boundary conditions. We have analyzed several quantities, such as the action-density profile, or some gauge invariant observables such as the Polyakov loop. After an appropriate reescaling taking into account the leading N dependence, the solutions show a universal pattern with a small remnant dependence on N that goes away in the large N limit. We have discussed how these new solutions relate to the constant curvature ones, that exist only for particlular values of the torus aspect ratios, suggesting that they could be obtained as smooth deformations of those along the lines presented in refs. [21, 22]. Finally, let us mention that we have payed particular attention to the Hamiltonian limit: $\mathbf{R} \times \mathbf{T}^3$, where these solutions represent tunneling events between two pure gauge configurations, essential to push the analytical perturbative domain beyond the small volume regime – see i.e. [23–26] and references therein.

Acknowledgments

References

[1] G. 't Hooft, *A Property of Electric and Magnetic Flux in Nonabelian Gauge Theories*, *Nucl. Phys. B* **153** (1979) 141–160.

[2] G. 't Hooft, *Some Twisted Selfdual Solutions for the Yang-Mills Equations on a Hypertorus*, *Commun. Math. Phys.* **81** (1981) 267–275.

[3] P. van Baal, *Some Results for SU(N) Gauge Fields on the Hypertorus*, *Commun. Math. Phys.* **85** (1982) 529.

[4] J. Dasilva Golán and M. García Pérez, "SU(N) fractional instantons and the Fibonacci sequence," [arXiv:2208.07133 [hep-th]].

[5] M. García Pérez, A. González-Arroyo and B. Soderberg, *Minimum Action Solutions for SU(2) Gauge Theory on the Torus With Nonorthogonal Twist*, *Phys. Lett. B* **235** (1990) 117–123.

[6] M. García Pérez, A. González-Arroyo, A. Montero and C. Pena, *Yang-Mills classical solutions and fermionic zero modes from lattice calculations*, *Nucl. Phys. B Proc. Suppl.* **63** (1998) 501–503, [`hep-lat/9709107`].

[7] A. Montero, *Numerical analysis of fractional charge solutions on the torus*, *JHEP* **05** (2000) 022, [`hep-lat/0004009`].

[8] A. González-Arroyo and A. Montero, *Selfdual vortex - like configurations in SU(2) Yang-Mills theory*, *Phys. Lett. B* **442** (1998) 273–278, [`hep-th/9809037`].

[9] A. Montero, *Vortex configurations in the large N limit*, *Phys. Lett. B* **483** (2000) 309–314, [`hep-lat/0004002`].

[10] A. González-Arroyo and M. Okawa, *The Twisted Eguchi-Kawai Model: A Reduced Model for Large N Lattice Gauge Theory*, *Phys. Rev. D* **27** (1983) 2397.

[11] M. García Pérez, A. González-Arroyo and M. Okawa, *Volume independence for Yang–Mills fields on the twisted torus*, *Int. J. Mod. Phys. A* **29** (2014) 1445001, [`1406.5655`].

[12] M. García Pérez, *Prospects for large N gauge theories on the lattice*, *PoS* **LATTICE2019** (2020) 276, [2001.10859].

[13] T. Ishikawa and M. Okawa, talk given by T. Ishikawa at the annual meeting of Japan Physics Society, Sendai, Japan, March 2003.

[14] W. Bietenholz, J. Nishimura, Y. Susaki and J. Volkholz, *A Non-perturbative study of 4-D U(1) non-commutative gauge theory: The Fate of one-loop instability*, *JHEP* **10** (2006) 042, [hep-th/0608072].

[15] M. Teper and H. Vairinhos, *Symmetry breaking in twisted Eguchi-Kawai models*, *Phys. Lett. B* **652** (2007) 359–369, [hep-th/0612097].

[16] T. Azeyanagi, M. Hanada, T. Hirata and T. Ishikawa, *Phase structure of twisted Eguchi-Kawai model*, *JHEP* **01** (2008) 025, [0711.1925].

[17] Z. Guralnik, R. C. Helling, K. Landsteiner and E. López, *Perturbative instabilities on the noncommutative torus, Morita duality and twisted boundary conditions*, *JHEP* **05** (2002) 025, [hep-th/0204037].

[18] A. González-Arroyo and M. Okawa, *Large N reduction with the Twisted Eguchi-Kawai model*, *JHEP* **07** (2010) 043, [1005.1981].

[19] F. Chamizo and A. González-Arroyo, *Tachyonic instabilities in 2 + 1 dimensional Yang–Mills theory and its connection to number theory*, *J. Phys. A* **50** (2017) 265401, [1610.07972].

[20] M. García Pérez, A. González-Arroyo, M. Koren and M. Okawa, *The spectrum of 2+1 dimensional Yang-Mills theory on a twisted spatial torus*, *JHEP* **07** (2018) 169, [1807.03481].

[21] A. González-Arroyo, *Constructing SU(N) fractional instantons*, *JHEP* **02** (2020) 137, [1910.12565].

[22] M. García Pérez, A. González-Arroyo and C. Pena, *Perturbative construction of selfdual configurations on the torus*, *JHEP* **09** (2000) 033, [hep-th/0007113].

[23] M. García Pérez, A. González-Arroyo and A. Sastre, *From confinement to adjoint zero-modes*, *eCONF* **C0906083** (2009) 06, [1003.5022].

[24] RTN collaboration, M. García Pérez et al., *Instanton like contributions to the dynamics of Yang-Mills fields on the twisted torus*, *Phys. Lett. B* **305** (1993) 366–374, [hep-lat/9302007].

[25] M. García Pérez, A. González-Arroyo and P. Martínez, *From perturbation theory to confinement: How the string tension is built up*, *Nucl. Phys. B Proc. Suppl.* **34** (1994) 228–230, [hep-lat/9312066].

[26] P. van Baal, *QCD in a finite volume*, In: At The Frontier of Particle Physics, pp. 683-760 (2001), hep-ph/0008206.